Cement & Concrete Composites 34 (2012) 684–691

Contents lists available at SciVerse ScienceDirect

Cement & Concrete Composites

journal homepage: www.elsevier.com/locate/cemconcomp

Rheological and hydration characterization of calcium sulfoaluminate cement pastes

Marta García-Maté [a], Isabel Santacruz [a], Ángeles G. De la Torre [a], Laura León-Reina [b], Miguel A.G. Aranda [a,*]

[a] Departamento de Química Inorgánica, Cristalografía y Mineralogía, Universidad de Málaga, 29071 Málaga, Spain
[b] Servicios Centrales de Investigación, Universidad de Málaga, 29071 Málaga, Spain

ARTICLE INFO

Article history:
Received 20 October 2011
Received in revised form 13 January 2012
Accepted 18 January 2012
Available online 1 February 2012

Keywords:
Rheology
Hydration
X-ray diffraction
Compressive strength
Cement paste
Sulfoaluminate

ABSTRACT

Calcium sulfoaluminate (CSA) cements are currently receiving a lot of attention because their manufacture produces less CO_2 than ordinary Portland cement (OPC). However, it is essential to understand all parameters which may affect the hydration processes. This work deals with the study of the effect of several parameters, such as superplasticizer (SP), gypsum contents (10, 20 and 30 wt.%) and w/c ratio (0.4 and 0.5), on the properties of CSA pastes during early hydration. This characterization has been performed through rheological studies, Rietveld quantitative phase analysis of measured X-ray diffraction patterns, thermal analysis and mercury porosimetry for pastes, and by compressive strength measurements for mortars. The effect of the used SP on the rheological properties has been established. Its addition makes little difference to the amount of ettringite formed but strongly decreases the large pore fraction in the pastes. Furthermore, the SP role on compressive strength is variable, as it increases the values for mortars containing 30 wt.% gypsum but decreases the strengths for mortars containing 10 wt.% gypsum.

1. Introduction

Calcium sulfoaluminate (CSA) cements are receiving increasing attention nowadays since their manufacture produces less CO_2 than ordinary Portland cement (OPC) [1–4]. These binders may have quite variable compositions, but all of them contain Ye'elimite phase, also called Klein's salt or tetracalcium trialuminate sulfate ($C_4A_3\underline{S}$) [5]. Cement nomenclature will be used hereafter C = CaO, S = SiO_2, A = Al_2O_3, F = Fe_2O_3, $\underline{S}$ = SO_3, M = MgO, T = TiO_2 and H = H_2O. The term CSA cements is usually reserved for those clinkers containing more than 50 wt.% of Klein's salt and they may also have minor amount of phases such as C_2S, CA, C_4AF, CS, $C\underline{S}H_2$, and so on [6]. Cements with large amounts of Ye'elimite may have special applications such as high strength developments at early-ages [7,8] and radioactive element encapsulation in a high-density cement paste [9,10]. On the other hand, a new related type of cement is emerging, aimed to replace OPC in the long term by combining approximately 20–30 wt.% of Ye'elimite (for early-age strength development) and 50–60 wt.% of activated belite (for medium-age strength development) [11–13]. This type of cement, initially developed in China but without the key activation of belite, is known as sulfobelite and also as belite-calcium sulfoaluminate cement to stress the importance of belite in its composition and performance.

CSA cements are prepared by mixing the clinker with different amounts of a calcium sulfate set regulator such as gypsum, bassanite or natural anhydrite, or mixtures of them. Their main properties are high early strengths, short setting times, impermeability, sulfate and chloride corrosion resistance and low alkalinity [5]. The early hydration of the CSA cements is mainly governed by the amount and reactivity of the added calcium sulfate [8,14–16]; it gives as main crystalline phases ettringite and monosulfate [17] and most of the hydration heat is released during the first 12–24 h of hydration [18]. The w/c ratio needed for full hydration is higher than that for an OPC. For instance, pure Ye'elimite reacting with the stoichiometric amount of anhydrite to yield ettringite requires a 0.78 w/c ratio [17,19] which may yield pastes with larger pore diameters than OPC pastes. Moreover, both high and low w/c ratios may involve severe expansion [20] with high w/c ratios also resulting in final strength development problems [21]; however, lower particle size [20] or the use of additives may eliminate some of these undesirable properties [22].

The dispersion of agglomerated cement particles is a key point to improve the workability of concrete to obtain more homogeneous mixtures and to reduce the amount of mixing water [23,24]. This is the role of superplasticizers and their use has become a common practice in OPC. It has been demonstrated that a lower water demand, within certain limits, is related with improved mechanical properties [25,26]. This is because the adsorption of the superplasticizers onto the surface of cement particles causes the repulsion of the particles (electrostatic or electrosteric). This repulsion depends [23] on the type and amount of

* Corresponding author. Tel.: +34 952131874; fax: +34 952131870.
E-mail address: g_aranda@uma.es (M.A.G. Aranda).

0958-9465/$ - see front matter © 2012 Elsevier Ltd. All rights reserved.
doi:10.1016/j.cemconcomp.2012.01.008

superplasticizer and the composition of the cement powder, such as type and content of gypsum, alkalis content, specific surface area, particle size distribution and type of mineral additions.

Within our ongoing research project in sulfobelite cements, it is important to understand the rheological properties of pastes containing high amounts of Ye'elimite which produces high amounts of ettringite at early hydration ages. To do so, we have started a study with samples of even higher Ye'elimite contents, CSA cements. The objective of this work is to understand the effect of different parameters: w/c content, superplasticizer and gypsum content on the rheological behavior, hydratation process (es) and porosity of selected calcium sulfoaluminate cement pastes. Finally, the consequences of these variables on the early hydration age mechanical properties of the corresponding mortars are discussed.

2. Material and methods

2.1. Material

2.1.1. Anhydrous cements

Calcium sulfoaluminate clinker (CS10), industrially produced in China and marketed in Europe by BELITH S.P.R.L. (Belgium), was used. Table 1 gives CS10 elemental analysis for the fused sample as determined by X-ray fluorescence (XRF) in a Magic X spectrometer (PANalytical, Almelo, The Netherlands) using the calibration curve of silica–alumina materials. The mineralogical composition of the as-received powder was determined by Rietveld methodology [27]: 72.3(1) wt.% of $C_4A_3\underline{S}$, 14.5(2) wt.% of β-C_2S, 6.8(1) wt.% of CT, 2.5(2) wt.% of C_4AF, 1.6(1) wt.% of M, 1.4(1) wt.% of C_2MS_2 and 0.9(1) wt.% of $C\underline{S}$. Calcium sulfoaluminate cements were prepared by mixing clinkers with different dosages of commercial micronized natural gypsum also marketed by BELITH S.P.R.L. (Belgium). The elemental composition of this $C\underline{S}H_2$, also determined by XRF, is given in Table 1. The added amounts of gypsum were 10, 20 and 30 wt.%. The cements are hereafter labeled as CS10-X, where X = 10, 20 or 30 stands for the amount of gypsum added to the clinkers. The Blaine fineness values determined for CS10 and gypsum were 480 and 500 m^2/kg, respectively. So, all blended cements showed Blaine values close to 480 m^2/kg. The OPC cement used for the strength measurements was a CEM I 52.5R from "Sociedad Financiera y Minera – Malaga plant (Spain)".

2.1.2. Cement pastes

Cement pastes were prepared with distilled water and CS10-X at w/c ratios of 0.5 and 0.4. A commercial polycarboxylate-based superplasticizer, Floadis 1623 (Adex Polymer S.L., Madrid, Spain), with a 25 wt.% of active matter, was added when appropriate. This superplasticizer is hereafter called SP. The added amount (ranging between 0 and 0.4 wt.%) is given as the percentage of active matter in the superplasticizer on a dry solid basis. The pastes were mechanically stirred with helices according to the EN196-3:2005 standard procedure. Bleeding was not observed for optimum or lower SP contents.

Table 1
Elemental composition (wt.%) of the raw materials determined by X-ray fluorescence.

	CS10	Gypsum
Al_2O_3	33.80	0.47
CaO	41.80	40.00
Fe_2O_3	2.37	0.15
K_2O	0.25	0.07
SiO_2	8.20	0.94
MgO	2.73	0.13
P_2O_5	0.13	0.56
TiO_2	1.50	–
SO_3	8.80	54.49
SrO	0.15	3.05
B_2O_3	–	–
Cr_2O_3	0.02	–
MnO	0.01	–
ZrO_2	0.07	–
Na_2O	<0.08	0.26

2.1.3. Quantitative phase analysis of pastes

An internal standard, ZnO (99.99%, Sigma–Aldrich, St. Louis, MO, USA), was added to the cements to a total content of 25 wt.% to perform the Rietveld quantitative phase analysis of the hydration products [28]. Pastes were cured at 20 ± 1 °C and 99% relative humidity (RH) for 3, 7 and 28 days. These samples were milled to a fine powder in an agate mortar before any diffraction measurement.

2.1.4. Compressive strengths

Standard mortars were prepared with water/cement/sand ratio of X/1/3 (X = 0.5 and 0.6) and mechanically homogenized according to EN196-1. The w/c ratios for mortars were slightly higher than for pastes in order to achieve a good homogenization. Prismatic samples of 40 × 40 × 160 mm (for OPC) and 30 × 30 × 30 mm (for OPC and CSA) were cast in a jolting apparatus (Model UTCM-0012, 3R, Montauban, France) with a total of 60 knocks. For a better homogenization, molds were first cast halfway and knocked 30 times. After that, they were fully cast and another 30 knocks were performed. The casts were cured at 20 ± 1 °C and 99% RH during 24 h. After that time, the samples were demolded and cured within a water bath at 20 ± 1 °C until measurements were performed. Compressive strengths of mortars were measured (Model Autotest 200/10 W, Ibertest, Madrid, Spain) at 3 and 7 days and the reported values are the average of 3 broken cubes. For OPC prismatic samples, the reported compressive strength values are the average of two measurements.

2.2. Analytical techniques

2.2.1. Rheological behavior

Rheological measurements of the pastes were carried out using a viscometer (Model VT550, Thermo Haake, Karlsruhe, Germany) with a serrated coaxial cylinder sensor, SV2P, provided with a solvent trap to reduce evaporation. Flow curves were obtained with controlled rate (CR) measurements using a three-stage measuring program with a linear increase in the shear rate from 0 to 100 s^{-1} in 60 s, a plateau at 100 s^{-1} for 30 s, and a further decrease to zero shear rate in 60 s. Before starting the rheological measurement, the pastes were presheared for 30 s at 60 s^{-1}.

2.2.2. Laboratory X-ray powder diffraction (LXRPD)

All patterns were recorded on an X'Pert MPD PRO diffractometer (PANalytical) using strictly monochromatic CuKα_1 radiation (λ = 1.54059 Å) [Ge (1 1 1) primary monochromator] and working in reflection geometry ($\theta/2\theta$). The X-ray tube worked at 45 kV and 40 mA. The optics configuration was a fixed divergence slit (1/2°), a fixed incident antiscatter slit (1°), a fixed diffracted antiscatter slit (1/2°) and X'Celerator RTMS (Real Time Multiple Strip) detector, working in scanning mode with maximum active length. Data were collected from 5° to 70° (2θ) during ~2 h. The samples were rotated during data collection at 16 rpm in order to enhance particle statistics.

2.2.3. LXRPD data analysis

Powder patterns of anhydrous and hydrated mixtures were analyzed by the Rietveld method as implemented in the GSAS software package [29] by using a *pseudo*-Voigt peak shape function [30] with the asymmetry correction included [31] to obtain

Rietveld Quantitative Phase Analysis (RQPA). The refined overall parameters were: background coefficients, unit cell parameters, zero-shift error, peak shape parameters and phase fractions.

2.2.4. Thermal analysis

Differential Thermal Analysis (DTA) and Thermogravimetry (TGA) data were taken for hydrated pastes on a SDT-Q600 analyzer from TA instruments (New Castle, DE). The temperature was varied from RT to 800 °C at a heating rate of 5 °C/min. Measurements were carried out on samples in open platinum crucibles under air flow.

2.2.5. Mercury intrusion porosimetry

Cement pastes were cured at 20 ± 1 °C and 99% relative humidity (RH) for 7 days prior to measurement of the open porosity and pore size distribution (PSD) through mercury porosimetry (MP) using a Quantachrome (Autoscan 33, Boynton Beach, Florida, US) porosimeter. The assumed contact angle for data evaluation was 130°.

3. Results and discussion

3.1. Rheological behavior

The amount of superplasticizer added to the pastes was optimized through the study of their rheological behavior. Fig. 1 shows the flow curves of the cement pastes with 30, 20 and 10 wt.% gypsum (Fig. 1a–c, respectively) at a w/c ratio of 0.4 (CS10-X, w/c = 0.4) with different SP contents. The insets show an enlarged view of the same flow curves. In general, pastes (w/c = 0.4) without SP show a shear thinning behavior and high viscosity values (between 2.6 and 3 Pa s at 50 s^{-1}). The addition of a small amount of additive, e.g. 0.1 wt.%, reduces drastically the viscosity of the pastes (~0.2 Pa s at 50 s^{-1}). From the viscosity curves (not shown), it can be observed how deflocculated pastes show a Newtonian behavior at shear rates higher than 10 s^{-1}. Minimum viscosity values were obtained after the addition of 0.15, 0.15 and 0.20 wt.% SP for CS10-30, CS10-20 and CS10-10, respectively, although the difference in viscosity is not so remarkable. The gypsum content does not present an important effect on the viscosity of the pastes in the studied range. The selected SP amount for CS10-30, CS10-20 and CS10-10 pastes with w/c = 0.5 was 0.15, 0.15 and 0.20 wt.% SP, respectively.

3.2. RQPA of hydrated pastes after 3, 7 and 28 days

The mineralogical changes of the cement pastes with ongoing hydration were quantified by LXRPD. Tables 2 and 3 report direct RQPA results for anhydrous and hydrated cements (ZnO was used as an internal standard). Fig. 2a and b show the Rietveld plots for CS10-30 anhydrous cement and hydrating paste, respectively. The latter, which contains a w/c content of 0.5 and the optimized

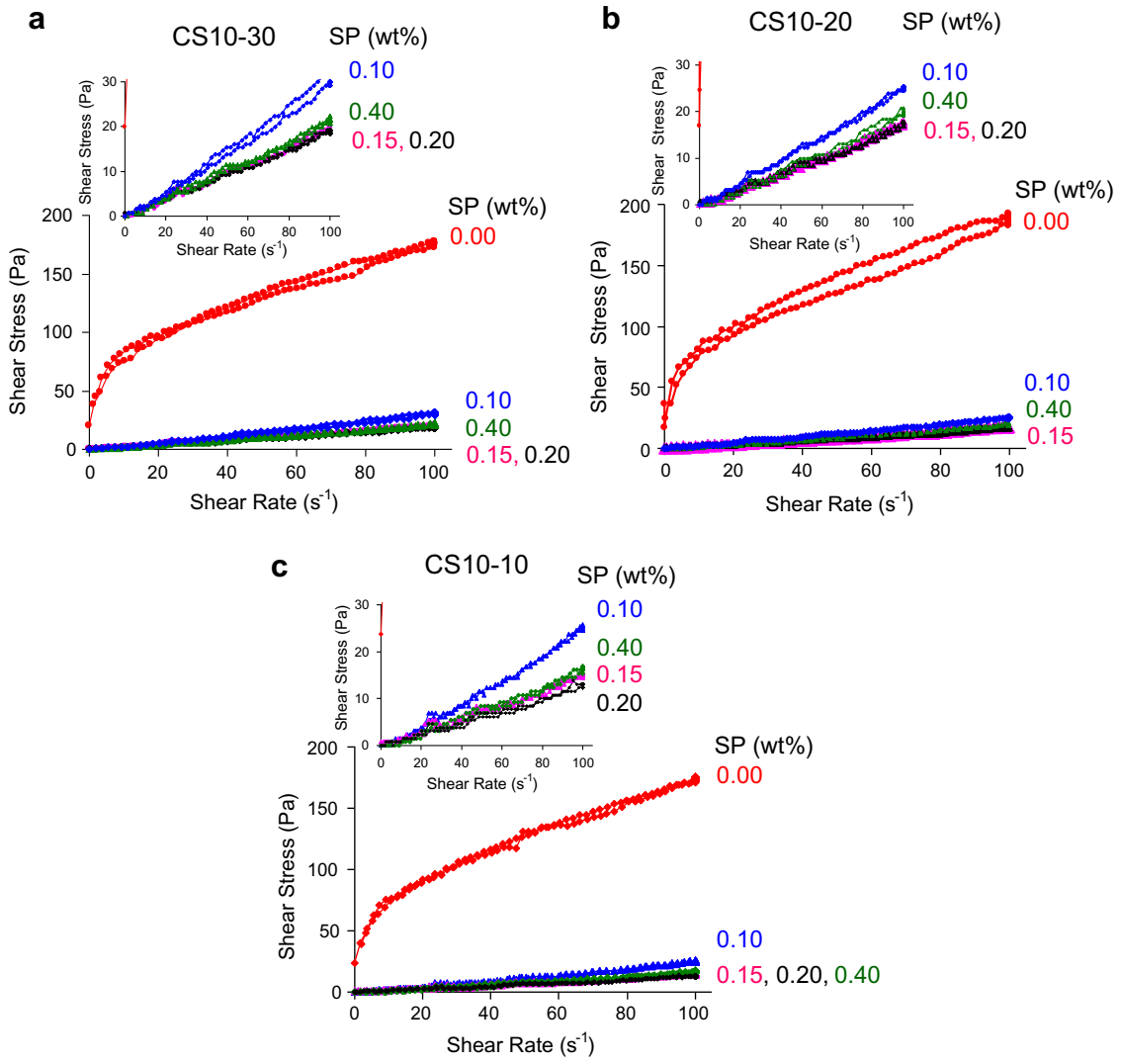

Fig. 1. Flow curves of CS10-30 (a), CS10-20 (b) and CS10-10 (c) pastes at w/c = 0.4 and different superplasticizer content. The insets show an enlarged view of the same flow curves.

Table 2
Direct RQPA results (wt.%) for anhydrous and hydrated (w/c = 0.4 and 0.5) CS10-30 cements (with and without superplasticizer). The numbers in parentheses are the standard deviations.

	Anhydrous	w/c = 0.4			w/c = 0.4, SP			w/c = 0.5, SP
	t_0	t_3	t_7	t_{28}	t_3	t_7	t_{28}	t_7
$C_4A_3\underline{S}$	33.4(2)	13.3(2)	10.4(2)	10.1(2)	15.0(2)	12.6(1)	9.3(2)	9.2(2)
$C\underline{S}H_2$	32.3(2)	12.4(2)	9.2(2)	9.4(2)	13.8(2)	12.5(1)	9.9(1)	13.7(2)
β-C_2S	2.8(2)	2.0(2)	2.0(2)	1.7(2)	2.2(2)	2.3(2)	1.4(1)	2.3(2)
$CaTiO_3$	1.3(1)	1.6(1)	1.5(1)	1.5(1)	1.6(1)	1.7(1)	1.3(1)	1.6(1)
MgO	0.7(1)	0.9(1)	1.0(1)	0.9(1)	0.9(1)	1.0(1)	0.7(1)	1.0(1)
AFt	–	40.5(2)	47.6(2)	48.2(2)	36.1(3)	40.6(2)	50.3(2)	39.4(3)
ZnO	29.5(1)	29.3(1)	28.3(1)	28.2(1)	30.4(1)	29.3(1)	27.1(1)	32.8(1)

Table 3
Direct RQPA results (wt.%) for anhydrous and hydrated (w/c 0.5) CS10-20 and CS10-10 cements after 0 days (anhydrous) and 7 days. The numbers in parentheses are the standard deviations.

	CS10-20				CS10-10			
	Anhydrous t_0	w/c = 0.4 t_7	w/c = 0.4, SP t_7	w/c = 0.5, SP t_7	Anhydrous t_0	w/c = 0.4 t_7	w/c = 0.4, SP t_7	w/c = 0.5, SP t_7
$C_4A_3\underline{S}$	39.1(2)	19.5(2)	18.3(2)	15.4(2)	46.9(2)	22.6(3)	24.5(3)	20.4(3)
$C\underline{S}H_2$	25.6(2)	7.3(2)	7.2(2)	5.3(2)	15.3(2)	1.4(2)	1.1(1)	1.1(1)
β-C_2S	3.2(2)	3.2(2)	2.7(2)	2.8(2)	3.6(2)	3.6(2)	3.7(2)	3.3(2)
$CaTiO_3$	1.9(2)	2.0(1)	1.9(1)	1.9(1)	2.3(1)	2.3(1)	2.4(1)	2.3(1)
MgO	0.8(1)	1.2(1)	1.1(1)	1.2(1)	1.2(1)	1.4(1)	1.4(1)	1.4(1)
AFt	–	34.0(3)	36.6(3)	42.2(3)	–	33.4(3)	33.0(2)	36.9(2)
ZnO	29.4(1)	32.8(1)	32.2(1)	31.2(1)	30.7(1)	35.3(1)	33.9(1)	34.6(1)

amount of SP, is shown after 7 days of hydration, as an example. From the data of the hydrated pastes shown in the tables, it can be observed that $C_4A_3\underline{S}$ and $C\underline{S}H_2$ contents decreased after 3, 7 and 28 days of hydration; the most important reduction was observed within the first 3 hydration days. Both phases were not fully reacted even after 28 days due to the added amount of water which is not enough for full reaction of all phases. High amounts of $C_6A\underline{S}_3H_{32}$ [ettringite or AFt phase] were present in all the pastes. The three main issues taking place during the hydration processes were: (i) disappearance of crystalline anhydrous phases, (ii) appearance of new phases, AFt and amorphous gels such as aluminate hydroxide hydrate (AH_3); and (iii) diminution of free water. Since direct RQPA results are normalized to 100 wt.% of crystalline phases, the percentage of the non-reactive phases, such as ZnO, is not constant due to the time-variation of the overall crystalline and amorphous phase ratio. Hence, in order to fully extract all the information about the hydration of cement pastes, direct RQPA results were normalized to include the amorphous phases and the free water content [17]. This methodology is based on the assumption that one crystalline phase remains inert during hydration. ZnO was used as this inert standard to normalize the amounts of the reacting phases according to expression 1:

$$\frac{\mathrm{ZnO}(t_y)_R}{C_4A_3\underline{S}(t_y)_R} = \frac{\mathrm{ZnO}(t_x)_N}{C_4A_3\underline{S}(t_x)_N - X} \quad (1)$$

where $\mathrm{ZnO}(t_y)_R$ and $C_4A_3\underline{S}(t_y)_R$ are the (Rietveld-calculated) percentages of those phases at time t_y. $\mathrm{ZnO}(t_x)_N$ and $C_4A_3\underline{S}(t_x)_N$ stand for percentages of these phases at normalized t_x, and X is the amount of $C_4A_3\underline{S}$ that has reacted at time ty ($t_x < t_y$). X is used to infer the amount of free water reacting and the amorphous phases formed according to the chemical reactions. For example, to obtain normalized RQPA at t_7 for CS10-30 pastes (w/c 0.5 and 0.15 wt.% SP) the normalized RQPA at t_0 (the previous time) is used. Thus, normalized phase assemblage at t_0 is: 24.3 wt.% of $C_4A_3\underline{S}$, 23.5 wt.% of gypsum, 2.0 wt.% of β-C_2S, 0.9 wt.% of $CaTiO_3$, 0.5 wt.% of MgO, 21.4 wt.% of ZnO and 27.3 wt.% of free water. Ettringite (AFt) is the only new crystalline phase, and $C_4A_3\underline{S}$ decreased during the hydration. This phase would react with gypsum and water according to:

$$C_4A_3\underline{S} + 2C\underline{S}H_2 + 34H \rightarrow C_6A\underline{S}_3H_{32} + 2AH_3 \quad (2)$$

This reaction corresponds to the formation of ettringite from Klein's salt [32] and it assumes that AH_3 is formed. However, crystalline AH_3 was not identified by XRPD. This phase is often reported [33] to be based on hydrous alumina using the term "AH_3" and it is considered as poorly-crystallized or amorphous phase.

The hydration reaction of belite may be quite different in OPC (Eq. (3)) [34] than in CSA cements (Eqs. (4) and (5)) [12,17,20,35]. After a careful examination of the pastes after 28 days hydration, no crystalline product arising from the hydration of belite was observed (portlandite, gehlenite hydrate and katoite). This behavior may be due to the low content of belite and its very low degree of reaction. Therefore, it was assumed that reaction (3) takes place and that the small amounts of CH and C–S–H phases were amorphous. It must be noted that the highest calculated amount of portlandite, according to Eq. (3), was 0.3 wt.%. For CSA cements, the Ca/Si ratio in C–S–H may be slightly lower than that in C–S–H from OPC, and consequently the amount of portlandite may be slightly higher. In any case, portlandite contents higher than 0.5 wt.% are not expected.

$$C_2S + 4.3H \rightarrow C_{1.7}SH_4 + 0.3CH \quad (3)$$

$$C_2S + AH_3 + 5H \rightarrow C_2ASH_8 \quad (4)$$

$$5C_2S + AH_3 + 17.2H \rightarrow C_3ASH_4 + C_{1.7}SH_4 + 0.2CH \quad (5)$$

Hence, using stoichiometric constraints [36,37] and the X value previously calculated (see Eq. (1)), the total amount of amorphous AH_3, C–S–H and CH was derived in each step. Finally, direct Rietveld results were recalculated as previously reported [36,37].

Tables 4 and 5 show the normalized results for anhydrous and hydrated cements. The theoretical total water content of the pastes is also given. We highlight that a w/c ratio of 0.5 would yield a total water content of 33.3 wt.%. However the presence of ZnO, added as internal standard, decreased this value down to 27.3 wt.% (see

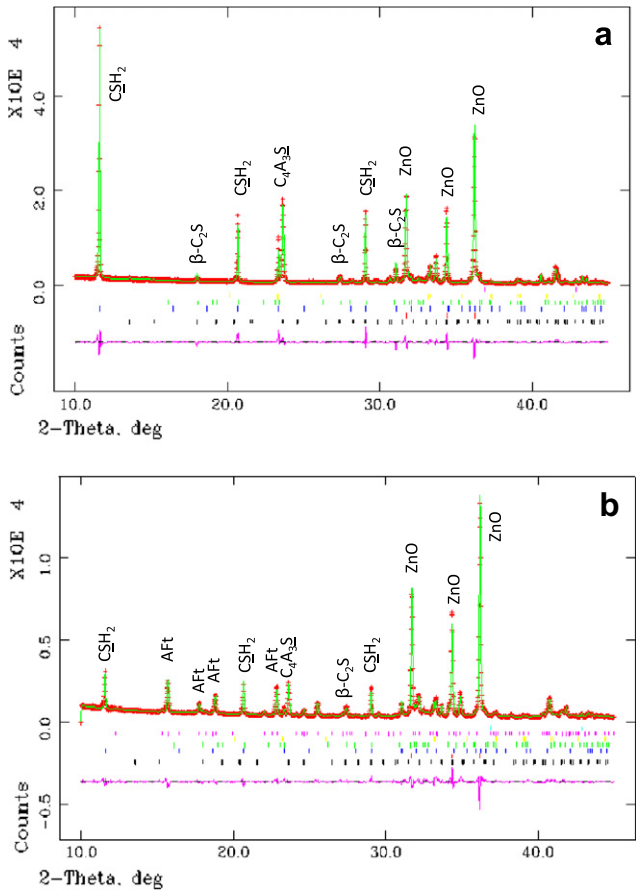

Fig. 2. Rietveld plot for anhydrous (a) and CS10-30 pastes (b). The latter contains w/c = 0.5 and superplasticizer and was studied after 7 days of hydration.

Tables 4 and 5). The total water content for every paste, measured by TG, is also shown in Tables 4 and 5 for comparison. The values confirm that water is not lost in our experimental conditions.

Fig. 3 shows the evolution of normalized phase content data (AFt and $C\underline{S}H_2$) for all the cement pastes after 7 days of hydration. The results agree well as larger amounts of ettringite are measured in samples with less amount of residual gypsum. In comparison to ordinary Portland cement, CSA cements react faster and most of the hydration heat occurs in the first day of hydration [18]. Ettringite is the main crystalline hydration product together with amorphous aluminum hydroxide. If gypsum is depleted, then monosulfate is formed according to Eq. (6). Furthermore, depending on the minor phases present in CSA cements, other hydration products may occur such as C–S–H phases, strätlingite, katoite, monocarboaluminate or hydrogarnet [38,39].

$$C_4A_3\underline{S} + 18H \rightarrow C_4A\underline{S}H_{12} + 2AH_3 \quad (6)$$

In the case of CS10-30 and CS10-20 pastes, $C_4A_3\underline{S}$ and gypsum content decreased but they were not depleted. The behavior of cement pastes with superplasticizer was not significantly different. It may be stated that reaction kinetics are slightly slowed down by SP (see Tables 4 and 5 and Fig. 3). The pastes with lower w/c ratio present lower degree of hydration, evident as larger amounts of $C_4A_3\underline{S}$ and gypsum and lower precipitation of ettringite are evolved. For CS10-10 pastes, $C_4A_3\underline{S}$ content was not depleted but gypsum content was practically exhausted. When gypsum was depleted, the hydration progressed by precipitation of calcium monosulfoaluminate hydrate (AFm). This was confirmed by DTA-TG (see below). The behavior of cement pastes with superplasticizer was not significantly different.

3.3. Thermal analysis

The changes of the cement pastes with ongoing hydration were also determined by DTA-TGA. Fig. 4a and b shows the DTA and TGA curves for CS10-30 and CS10-10 pastes (w/c = 0.5, SP), respectively, to highlight the role of the amount of gypsum on the hydration products. Both cement pastes were measured after 7 days of hydration as a representative example for all the compositions. The CS10-30 paste (Fig. 4a) shows an endothermic peak at ~100 °C (point 1) mainly due to the weight loss of water of ettringite [17] and a small endothermic peak ~125 °C (point 2), likely corresponding to the weight loss from gypsum [17]. The analysis of the CS10-10 paste also showed the same endothermic peak at ~100 °C (point 1). However the small endothermic peak at ~125 °C corresponding to the weight loss of gypsum is not observed, as this phase was exhausted during hydration. When gypsum is depleted, the hydration progresses by precipitation of calcium monosulfoaluminate hydrate (AFm) [17]. This is confirmed by the small peak which appears at ~150 °C (point 3), corresponding to this new phase. This peak is evident in Fig. 4b but not in Fig. 4a. Furthermore, the DTA curve for CS10-20 paste (w/c = 0.5, SP), not shown, does not display this endothermic peak. Finally, the broad endotherm centered close to 250 °C is likely associated to the loss of aluminate hydroxide hydrate gel water. The broad feature of this endotherm is consistent with the amorphous nature of this phase. We recall that crystalline gibbsite was not detected in any studied powder pattern.

3.4. Porosity characterization

Figs. 5a–c show the pore size distribution obtained by mercury porosimetry for the CS10-30, CS10-20 and CS10-10 pastes, respectively, at 7 days hydration (w/c ratios of 0.4 and 0.5 with and without SP). At the top of each panel, an enlarged view is also presented to highlight the consequences of the SP addition on the large-pores.

Table 4
Normalized data for CS10-30 pastes after 3, 7 and 28 hydration days. Theoretical total water, w_T^{th}, and total water contents determined from TG are also shown.

	w/c = 0.4				w/c = 0.4, SP				w/c = 0.5, SP	
	t_0	t_3	t_7	t_{28}	t_0	t_3	t_7	t_{28}	t_0	t_7
$C_4A_3\underline{S}$	33.6	14.9	11.7	11.2	33.6	16.8	14.2	10.1	30.9	10.1
$C\underline{S}H_2$	32.4	13.8	10.4	10.5	32.4	15.6	14.1	10.9	29.9	15.1
β-C_2S	2.8	2.3	2.4	2.0	2.8	2.4	2.6	1.6	2.5	2.6
$CaTiO_3$	1.3	1.7	1.7	1.8	1.3	1.7	1.9	1.4	1.2	1.8
MgO	–	–	–	–	–	–	–	–	0.6	1.1
Wf	29.9	9.8	7.1	6.6	29.9	11.1	9.2	5.8	34.9	11.8
AFt	–	45.5	53.5	54.0	–	40.9	45.6	55.4	–	43.3
Hydrated amorphous	–	12.0	13.2	13.9	–	11.5	12.4	14.8	–	14.2
w_T^{th}	–	TG, w_T = 26.2	TG, w_T = 28.6	TG, w_T = 28.6	–	TG, w_T = 26.3	TG, w_T = 26.5	TG, w_T = 28.6	–	TG, w_T = 26.9
23.1 for w/c = 0.4										
27.3 for w/c = 0.5										

Table 5
Normalized data for CS10-20 and CS10-10 pastes after 7 hydration days. Theoretical total water, w_T^{th}, and total water contents determined from TG are also shown.

	CS10-20						CS10-10					
	w/c = 0.4		w/c = 0.4, SP		w/c = 0.5, SP		w/c = 0.4		w/c = 0.4, SP		w/c = 0.5, SP	
	t_0	t_7	t_0	t_7	t_0	t_7	t_0	t_7	t_0	t_7	t_0	t_7
$C_4A_3\underline{S}$	38.8	22.8	38.8	21.3	36.1	16.7	47.1	28.3	47.1	29.4	43.9	23.5
$C\underline{S}H_2$	25.4	8.6	25.4	8.4	23.7	5.8	15.4	1.7	15.4	1.3	14.3	1.3
β-C_2S	3.2	3.7	3.2	3.2	2.9	3.1	3.7	4.5	3.7	4.5	3.4	3.8
$CaTiO_3$	1.9	2.4	1.9	2.2	1.8	2.0	2.4	2.9	2.4	2.8	2.2	2.7
MgO	0.8	1.4	0.8	1.2	0.8	1.3	1.2	1.7	1.2	1.7	1.2	1.7
Wf	29.9	8.7	29.9	7.4	34.7	12.6	30.2	2.4	30.2	5.1	35.0	8.5
AFt	–	39.8	–	42.7	–	45.5	–	41.9	–	39.7	–	42.3
Hydrated amorphous	–	12.6	–	13.6	–	13.0	–	16.6	–	15.5	–	16.2
w_T^{th} 23.1 for w/c = 0.4 27.3 for w/c = 0.5	–	TG, w_T = 21.2	–	TG, w_T = 23.5	–	TG, w_T = 26.4	–	TG, w_T = 23.3	–	TG, w_T = 21.3	–	TG, w_T = 26.4

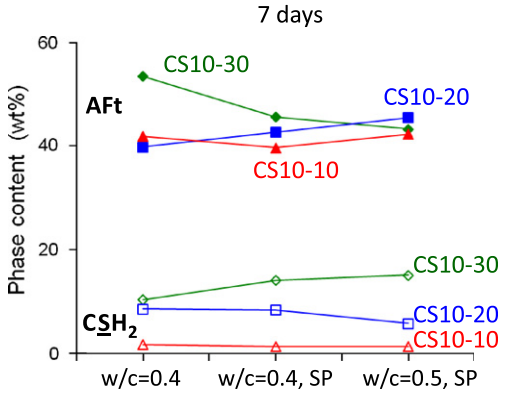

Fig. 3. Normalized values for AFt and $C\underline{S}H_2$ for all the studied pastes after 7 days hydration.

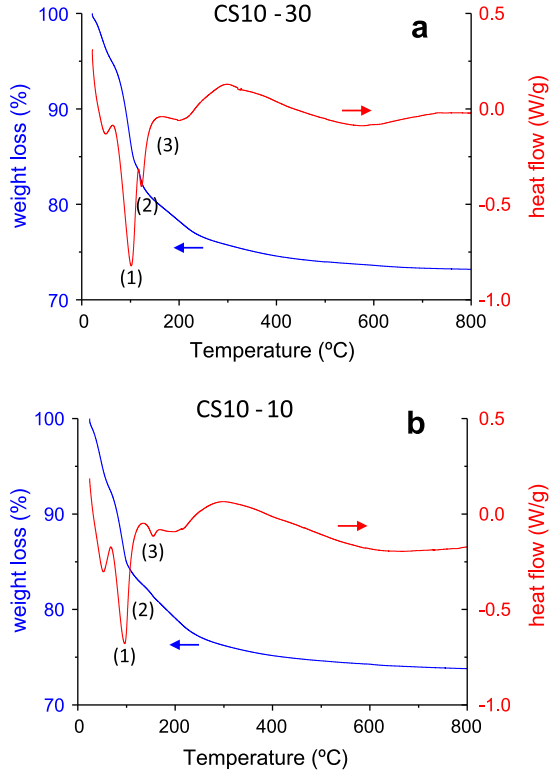

Fig. 4. DTA-TGA curves for CS10-30 (a) and CS10-10 (b) pastes after 7 days hydration.

Fig. 5a shows that CS10-30 paste with w/c = 0.4 and without SP shows a bimodal behavior with pores centered at 12 and 554 nm (see also Table 6). Higher amounts of water (w/c = 0.5) enlarge the average size of the pores to 21 and 677 nm, as expected. This bimodal behavior has been previously reported for CSA pastes [19]. The addition of SP slightly enlarges the small pore diameters (see Fig. 5a and Table 6) but strongly decreases the amount of the large pores (those with diameters close to 500 nm or larger).

CS10-20 and CS10-10 pastes present the same tendency in the pore size and pore size distribution. The increase in w/c ratio increases the size of the pores. Furthermore, the addition of superplasticizers strongly decreases (removes) the large pores and slightly increases the size of the nanometer-pores (see Table 6 and Fig. 5b and c).

Table 6 also reports the total open porosity for the studied pastes. As expected, the total open porosity increases with the w/c ratio (for a given gypsum content). Moreover the addition of a small amount of SP decreases the pastes open porosity for the studied w/c ratios. Therefore, SP addition may increase the durability and mechanical strength of the mortars as the reduction of porosity is a key for obtaining these objectives. Finally, Table 6 also shows the corresponding values for an OPC paste (w/c = 0.4) for the sake of comparison. The obtained values for OPC are in agreement with those previously reported in the literature [40].

3.5. Compressive strength measurements

The compressive strength measurements were carried out on small cubes, and an initial study was also carried out with CEM I 52.5 R mortars for the sake of comparison. For the latter, both cubes (30 × 30 × 30 mm) and prisms (40 × 40 × 160 mm) were produced. For the (OPC) prisms, the average compressive strengths were 48.8(9), 54.3(9) and 62.7(1.5) MPa, for 3, 7 and 28 days, respectively. For the small cubes, the corresponding values were 41.5(6), 50.6(7) and 54.7(1.9) MPa, for the same hydration ages.

Table 7 gives the compressive strength measurements for several CS10 pastes as described in the experimental section for small cubes (30 × 30 × 30 mm). The influence of water and gypsum contents of the mortars in the compressive strengths is interrelated. Hence, a full study varying both parameters has been carried out. From the analysis of the data reported in Table 7, it is clear that w/c = 0.5 mortars always yield higher strengths than the analogous w/c = 0.6 mortars. This is in agreement with the porosity study. Furthermore, the role of gypsum content is also very important as 30 wt.% yields an important decrease in the compressive strength values. This study shows that the optimum gypsum content to have the highest compressive strengths should be between 10 and 20 wt.%. This result is in full agreement with the RQPA of

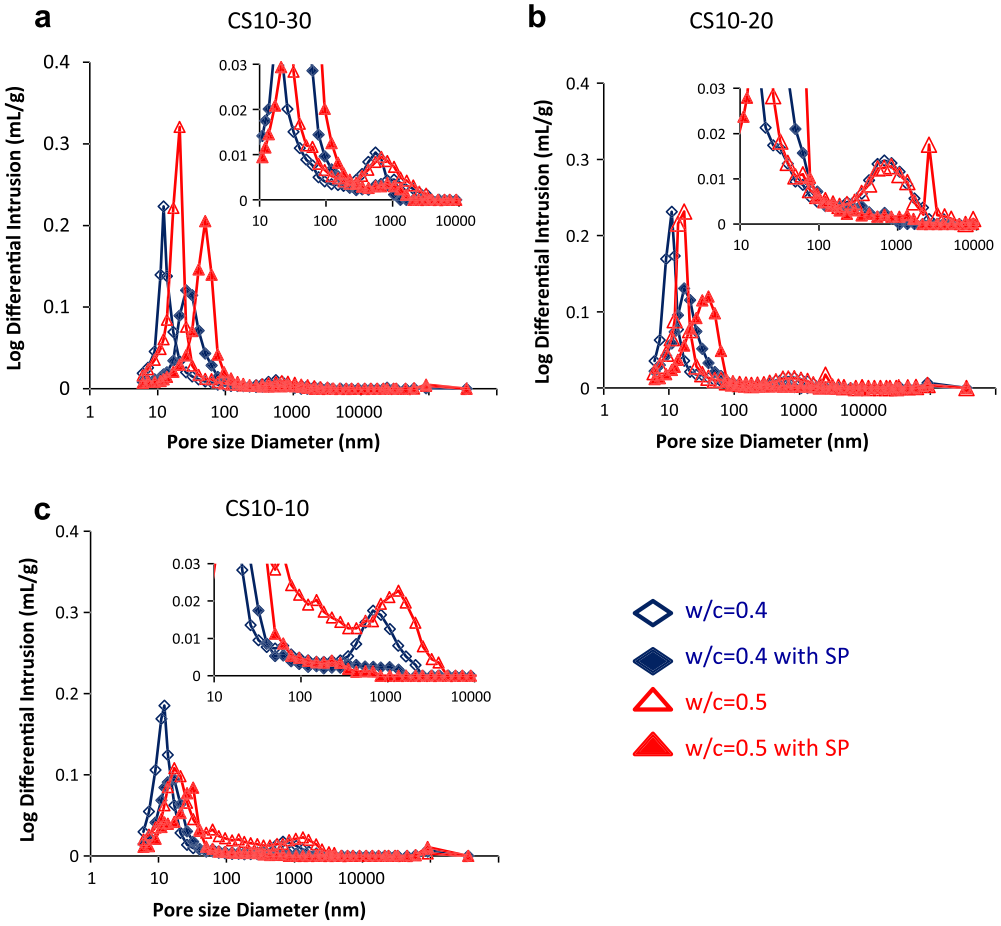

Fig. 5. Average pore diameter of the studied ceramic pastes. The insets show enlarged views of the large pore region.

Table 6
Percentage of porosity and average pore diameters for the studied pastes (7 days of hydration).

	Open porosity (vol.%)	Average "small" pore diameter (nm)	Average "large" pore diameter (nm)
OPC, w/c = 0.4	12.0	12	350
CS10-30, w/c = 0.4	11.5	12	554
CS10-30, w/c = 0.5	14.8	21	677
CS10-20, w/c = 0.4	14.4	11	676
CS10-20, w/c = 0.5	15.6	17	829
CS10-10, w/c = 0.4	13.7	12	678
CS10-10, w/c = 0.5	15.8	17	1329
CS10-30, w/c = 0.4, SP	10.8	26	–
CS10-30, w/c = 0.5, SP	14.1	50	–
CS10-20, w/c = 0.4, SP	13.3	17	–
CS10-20, w/c = 0.5, SP	13.6	40	–
CS10-10, w/c = 0.4, SP	9.9	17	–
CS10-10, w/c = 0.5, SP	9.6	26	–

Table 7
Compressive strength for CS10 mortar (cubes of 30 × 30 × 30 mm dimensions) at different hydration ages. The numbers in parentheses are the standard deviations.

	Strength – 3 days (MPa)	Strength – 7 days (MPa)
OPC, w/c = 0.5	41.5(0.6)	50.6(0.7)
CS10-30, w/c = 0.5	32.9(0.9)	40.6(1.0)
CS10-30, w/c = 0.6	32.2(0.2)	37.6(0.6)
CS10-20, w/c = 0.5	44.0(1.1)	47.5(1.4)
CS10-20, w/c = 0.6	36.7(0.3)	40.9(0.9)
CS10-10, w/c = 0.5	43.1(0.2)	50.0(0.6)
CS10-10, w/c = 0.6	34.5(0.4)	35.1(1.2)
CS10-30, w/c = 0.5, SP	36.7(1.2)	45.6(0.5)
CS10-30, w/c = 0.6, SP	33.3(0.2)	39.2(0.8)
CS10-20, w/c = 0.5, SP	44.9(0.2)	46.1(0.9)
CS10-20, w/c = 0.6, SP	36.1(0.4)	37.0(0.5)
CS10-10, w/c = 0.5, SP	38.1(0.8)	39.3(0.9)
CS10-10, w/c = 0.6, SP	34.9(0.6)	35.1(0.4)

the pastes, since gypsum is completely depleted in CS10-10 pastes but there is a significant remaining amount in CS10-20 pastes. It must be noted that CS10-10 and CS10-20 mortars with w/c ratio of 0.5 gave compressive strength values similar to those of OPC mortars, see Table 7.

Finally, from the data reported in Table 7, the role of SP in the compressive strengths may be discussed. The addition of this SP to CS10-30 mortars (both with w/c ratios of 0.5 and 0.6) slightly increases the compressive strengths. The addition of the SP to CS10-20 mortars makes very little change to this property irrespective of the w/c ratio. However, the addition of the SP to CS10-10 mortars makes little change for w/c = 0.6 but decreases the compressive strength for mortars with w/c = 0.5. More studies are needed to correlate the chemical nature of the superplasticizer with the water, gypsum and ettringite contents of the mortars.

4. Conclusions

Calcium sulfoaluminate cement pastes with different gypsum contents (10, 20 and 30 wt.%), w/c ratios (0.4 and 0.5), and with and without superplasticizer have been studied. The addition of a small amount of superplasticizer reduced considerably the viscos-

ity of the pastes (from 2.6–3.0 Pa s to 0.2 Pa s at 50 s^{-1}). In general, during hydration, most of the hydration heat evolution occurred at 7 days, and between 7 and 28 days hydration proceeded very slowly with very little changes. The evolution of all phases was studied by Rietveld quantitative phase analysis. $C_4A_3\underline{S}$ and gypsum decreased but their contents were not depleted for CS10-30 and CS10-20 pastes. The main crystalline phase formed during hydration is ettringite (AFt) and its variation could be determined. However, crystalline gibbsite is not detected and its content was indirectly determined through chemical constraints. Samples with higher gypsum content (30 wt.%) showed a weight loss at 125 °C (due to the remaining gypsum), which is negligible for CS10-10 pastes. When gypsum is depleted, the hydration progresses by precipitation of AFm which is evident in the DTA curves as a small endotherm centered at 150 °C. The average porous diameter and pore distribution are affected by the w/c ratio and superplasticizer presence. In the former, by increasing the w/c content, the porous diameter increases. In the later, the addition of SP to a paste with the same w/c changes the bimodal pore distribution to a monomodal one, eliminating the larger pores. Finally, the compressive strength measurements indicate that mortars with w/c ratio of 0.5 always gave higher values than those derived from mortars with w/c = 0.6 (e.g. 50.0(0.6) and 35.1(1.2) for CS10-10 with w/c 0.5 and 0.6, respectively, at 7 days hydration).

Acknowledgements

This work has been supported by Spanish Ministry of Science and Innovation through MAT2010-16213 research grant, which is co-funded by FEDER, and Ramón y Cajal Fellowship (RYC-2008-03523).

References

[1] Gartner E. Industrially interesting approaches to "low -CO_2" cements. Cem Concr Res 2004;34:1489–98.
[2] Sharp JH, Lawrence CD, Yang R. Calcium sulphoaluminate cements – Low-energy cements, special cements or what? Adv Cem Res 1999;11:3–13.
[3] Popescu CD, Muntean M, Sharp JH. Industrial trial production of low energy belite cement. Cem Concr Compos 2003;25:689–93.
[4] Feraille A, Alaoui A, Steckmeyer A, Le Roy R. New cements for sustainable development. In: Proceedings of 12th international congress on the chemistry of cement. Montreal, Canada; 2007.
[5] Odler I. Special inorganic cements. London: Taylor and Francis; 2000.
[6] Sahu S, Majling J. Phase compatibility in the system CaO–SiO_2–Al_2O_3–Fe_2O_3–SO_3 referred to sulphoaluminate belite cement clinker. Cem Concr Res 1993;23:1331–9.
[7] Quillin K. Performance of belite–sulfoaluminate cements. Cem Concr Res 2001;31:1341–9.
[8] Glasser FP, Zhang L. High-performance cement matrices based on calcium sulphoaluminate-belite compositions. Cem Concr Res 2001;31:1881–6.
[9] Cau dit Coumes C, Courtois S, Peysson S, Ambroise J, Péra J. Calcium sulfoaluminate cement blended with OPC: a potential binder to encapsulate low-level radioactive slurries of complex chemistry. Cem Concr Res 2009;39:740–7.
[10] Zhou Q, Milestone NB, Hayes M. An alternative to Portland cement for waste encapsulation—the calcium sulfoaluminate cement system. J Hazard Mater 2006;136:120–9.
[11] Gartner E, Li GS. High-belite sulfoaluminate clinker: fabrication process and binder preparation. World Patent Application WO 2006/018569 A2.
[12] Cuberos AJM, de la Torre AG, Álvarez-Pinazo G, Martín-Sedeño MC, Schollbach K, Pöllmann H, et al. Active iron-rich belite sulfoaluminate cements: clinkering and hydration. Environ Sci Technol 2010;44:6855–62.
[13] Morin V, Walenta G, Gartner E, Termkhajornkit P, Baco I, Casabonne JM. Hydration of a belite-calcium sulfoaluminate- ferrite cement: Aether™. In: Proceedings of the 13th international congress on the chemistry of cement. Madrid, Spain; 2011.
[14] Péra J, Ambroise J. New applications of calcium sulphoaluminate cement. Cem Concr Res 2004;34:671–6.
[15] Sahu S, Havlica J, Tomková V, Majling J. Hydration behaviour of sulphoaluminate belite cement in the presence of various calcium sulphates. Thermochim Acta 1991;175:45–52.
[16] Marchi M, Costa U. Influence of the calcium sulphate and W/C ratio on the hydration of calcium sulphoaluminate cement. In: Proceedings of the 13th international congress on the chemistry of cement. Madrid, Spain; 2011.
[17] Winnefeld F, Lothenbach B. Hydration of calcium sulphoaluminate cements-experimental findings and thermodynamic modelling. Cem Concr Res 2010;40:1239–47.
[18] Zhang L, Glasser FP. Hydration of calcium sulphoaluminate cements at less than 24 h. Avd Cem Res 2002;14:141–55.
[19] Bernardo G, Telesca A, Valenti GL. A porosimetric study of calcium sulfoaluminate cement pastes cured at early ages. Cem Concr Comp 2006;36:1042–7.
[20] Chen IA, Hargis CW, Juenger MCG. Understanding expansion in calcium sulfoaluminate-belite cements. Cem Concr Res 2012;42:51–60.
[21] Ambroise J, Georgin JF, Peysson S, Péra J. Influence of polyether polyol on the hydration and engineering properties of calcium sulphoaluminate cement. Cem Concr Comp 2009;31:474–82.
[22] Chang W, Li H, Wei M, Zhu Z, Zhang J, Pei M. Effects of polycarboxylic acid based superplasticiser on properties of sulphoaluminate cement. Mater Res Innovations 2009;13:7–10.
[23] Palacios M, Houst YF, Bowen P, Puertas F. Adsorption of superplasticizer admixtures on alkali-activated slag pastes. Cem Concr Res 2009;39:670–7.
[24] Papo A, Piani L. Effect of various superplasticizers on the rheological properties of Porlant cement pastes. Cem Concr Res 2004;34:2097–101.
[25] Björnstrom J, Chandra S. Effect of superplasticizers on the rheological properties of cements. Mat Struct 2003;36:685–92.
[26] Puertas F, Santos H, Palacios M, Martínez-Ramírez S. Polycarboxylate superplasticizer admixtures: effect on hydration, microstructure and rheological behaviour in cement pastes. Adv Cem Res 2005;17:77–89.
[27] Rietveld HM. A profile refinement method for nuclear and magnetic structures. J Appl Crystallogr 1969;2:65–71.
[28] De la Torre AG, Bruque S, Aranda MAG. Rietveld quantitative amorphous content analysis. J Appl Crystallogr 2001;34:196–202.
[29] Larson AC, Von Dreele RB. General structure analysis system (GSAS). Los Alamos National Laboratory Report LAUR; 2000. p. 86–748.
[30] Thompson P, Cox DE, Hasting JB. Rietveld refinement of Debye-Scherrer synchrotron X-ray data from Al_2O_3. J Appl Crystallogr 1987;20:79–83.
[31] Finger LW, Cox DE, Jephcoat AP. A correction for powder diffraction peak asymmetry due to diaxial divergence. J Appl Crystallogr 1994;27:892–900.
[32] Meller N, Hall C, Jupe AC, Colston SL, Jacques SDM, Barnes P, et al. The paste hydration of brownmillerite with and without gypsum: a time resolved synchrotron diffraction study at 30, 70, 100 and 150 °C. J Mater Chem 2004;14:428–35.
[33] Scrivener KL, Capmas A. Calcium aluminate cements, Leás chemistry of cement and concrete; 1998 [Chapter 13].
[34] Scrivener KL, Fullmann T, Gallucci E, Walenta G, Bermejo E. Quantitative study of Portland cement hydration by X-ray diffraction/Rietveld analysis and independent methods. Cem Concr Res 2004;34:1541–7.
[35] Juenger MCG, Winnefeld F, Provis JL, Ideker JH. Advances in alternative cementitious binders. Cem Concr Res 2011;41:1232–43.
[36] Martín-Sedeño MC, Cuberos AJM, De la Torre AG, Álvarez-Pinazo G, Ordónez LM, Gateshki M, et al. Aluminum-rich belite sulfoaluminate cements: clinkering and early age hydration. Cem Concr Res 2010;40:359–69.
[37] Cuberos AJM, De la Torre AG, Martín-Sedeño MC, Moreno-Real L, Merlini M, Ordónez LM, et al. Phase development in conventional and active belite cement pastes by Rietveld analysis and chemical constraints. Cem Concr Res 2009;39:833–42.
[38] Glasser FP, Zhang L. High-performance cement matrices based on calcium sulfoaluminate-belite compositions. Cem Concr Res 2001;21:1881–6.
[39] Li GS, Walenta G, Gartner EM. Formation and hydration of low CO_2 cements based on belite, calcium sulphoaluminate and calcium aluminoferrite. In: Proceedings of the 12th international congress on the chemistry of cement. Montreal, Canada; 2007.
[40] Pandey SP, Sharma RL. The influence of mineral additives on the strength and porosity of OPC mortar. Cem Concr Res 2000;30:19–23.